The Journal of Experimental Biology 213, 2808-2819

doi:10.1242/jeb.042150

Development of a dopaminergic system in sea urchin embryos and larvae

Hideki Katow[1,*], Takashi Suyemitsu[2], Shio Ooka[1], Junko Yaguchi[3], Takayuki Jin-nai[2], Iku Kuwahara[2], Tomoko Katow[1], Shunsuke Yaguchi[3] and Hirokazu Abe[1]

[1]Research Center for Marine Biology, Tohoku University, Asamushi, Aomori, Aomori 039-3501, Japan, [2]Department of Regulation Biology, Faculty of Science, Saitama University, Saitama-ku, Saitama 338-8570, Japan and [3]Shimoda Marine Research Center, University of Tsukuba, Shizuoka 415-0025, Japan

*Author for correspondence (hkatow@m.tohoku.ac.jp)

Accepted 6 May 2010

SUMMARY

The mechanisms that regulate the organized swimming movements of sea urchin blastulae are largely unknown. Using immunohistochemistry, we found that dopamine (DA) and the *Hemicentrotus pulcherrimus* homolog of the dopamine receptor D1 (Hp-DRD1) were strongly co-localized in 1–2 μm diameter granules (DA/DRD1 granules). Furthermore, these granules were arranged across the entire surface of blastulae as they developed locomotory cilia before hatching, and remained evident until metamorphosis. DA/DRD1 granules were associated with the basal bodies of cilia, and were densely packed in the ciliary band by the eight-arm pluteus stage. The transcription of *Hp-DRD1* was detected from the unfertilized egg stage throughout the period of larval development. Treatment with *S*-(–)-carbidopa, an inhibitor of aromatic-L-amino acid decarboxylase, for 20–24 h (i) from soon after insemination until the 20 h post-fertilization (20 hpf) early gastrula stage and (ii) from the 24 hpf prism larva stage until the 48 hpf pluteus stage, inhibited the formation of DA granules and decreased the swimming activity of blastulae and larvae in a dose-dependent manner. Exogenous DA rescued these deprivations. The formation of DRD1 granules was not affected. However, in 48 hpf plutei, the serotonergic nervous system (5HT-NS) developed normally. Morpholino antisense oligonucleotides directed against *Hp-DRD1* inhibited the formation of DRD1 granules and the swimming of larvae, but did not disturb the formation of DA granules. Thus, the formation of DRD1 granules and DA granules occurs chronologically closely but mechanically independently and the swimming of blastulae is regulated by the dopaminergic system. In plutei, the 5HT-NS closely surrounded the ciliary bands, suggesting the functional collaboration with the dopaminergic system in larvae.

Supplementary material available online at http://jeb.biologists.org/cgi/content/full/213/16/2808/DC1

Key words: preneural, dopamine, dopamine receptor D1, ciliary bands, embryonic swimming, larval swimming, sea urchin embryos.

INTRODUCTION

The swimming of marine larvae depends on ciliary propulsion and is critically important for feeding, escape responses (Strathmann, 2007; Stephens, 2008) and photosensitive vertical migration (Ooka et al., 2010). In sea urchin embryos, motile cilia are evident from the blastula stage, and rotatory movement by embryos can be observed in the fertilization envelope. Serotonin plays a role in the regulation of the beating of larval cilia (Yaguchi and Katow, 2003; Katow et al., 2009). However, its role in the regulation of the cilia of blastulae is unknown. The swimming activity of hatched blastulae is insensitive to *para*-chlorophenylalanine (*p*CPA), a potent inhibitor of tryptophan 5-hydroxylase, and the serotonergic nervous system (5HT-NS) is not yet formed at this stage (Yaguchi and Katow, 2003). Nevertheless, the swimming behavior of blastulae is organized to a considerable degree. For instance, sea urchin blastulae can swim by orienting their long apical tuft cilia in the target direction (Soliman, 1983a; Stephens, 2008). This suggests that swimming in sea urchin blastulae might be regulated by a distinctive mechanism that is not related to the 5HT-NS.

The beating of cilia is known to be regulated by catecholamines, in particular dopamine (DA) in invertebrates (Soliman, 1983b; Voronezhskaya et al., 1999; Martin et al., 2008) and vertebrates (Maruyama et al., 1983; Tomé et al., 2007). To date, expression of catecholamines has been demonstrated in basic deuterostomes, including asteroidae (Huet and Fraquinet, 1981), brittlestars (De Bremaeker et al., 2000) and holothurian species (Inoue et al., 2002), but not in hemichordates. For instance, embryos of *Lytechinus pictus* express DA from the 18 h post-fertilization (hpf) swimming blastula stage, as detected by high-performance liquid chromatography with electrochemical detection. This is followed by a period when DA is undetectable from the 28 hpf mesenchyme blastula stage to the 42 hpf late gastrula stage, and trace amounts can be found in 49 hpf late prism larvae (Anitole-Misleh and Brown, 2004). Furthermore, in *Strongylocentrotus droebachiensis*, DA is only present at the larval stages, as demonstrated by immunohistochemistry (Bisgrove and Burke, 1987). It is possible that catecholamines are involved in morphogenesis during the early development of sea urchins, *Psammechinus miliaris* (Gustafson and Toneby, 1970; Toneby, 1980; Anitole-Misleh and Brown, 2004). However, the time lag between the onset of embryonic swimming and the immunohistological appearance of dopaminergic cells in larvae suggests the presence of preneural dopaminergic regulation of the beating of the cilia of blastulae.

DA has been shown to signal to the cytoplasm of embryonic cells through DA receptors, which are a group of metabotropic G-protein-coupled receptors (GPCRs) (Girault and Greengard, 2004). Microarray analysis of the expression of *DA receptor D1* (*Sp-DRD1*) and *DA receptor D2* (*Sp-DRD2*) in *Strongylocentrotus purpuratus* has revealed that the mRNAs are expressed from the two-cell stage to the early prism stage. This suggests that DA functions during early development in this species (Sea Urchin Genome Project, http://www.spbase.org/SpBase/search/anno_search_result.php).

Despite previous biochemical observations that suggest a role for DA in sea urchin embryogenesis (Gustafson and Toneby, 1970; Toneby, 1980; Capasso et al., 1987; Carginale et al., 1995; Anitole-Misleh and Brown, 2004) and embryonic swimming activity (Soliman, 1983a), few morphological studies exist to support this. Therefore, in this study we investigated the localization of DA and its receptor Hp-DRD1, a D1 homolog found in the sea urchin species *Hemicentrotus pulcherrimus* (Suyemitsu, 2007) (*Hp-DRD1*; accession number AB510005, see supplementary material Fig. S1), from the pre-hatched blastula stage to metamorphosis using whole-mount immunohistochemistry. To determine whether DA might play a role in swimming behavior, the expression and sub-cellular localization of DA and Hp-DRD1 were examined by immunostaining for DA and Hp-DRD1, as well as for markers of the serotonergic system. In addition, pharmacological and gene knockdown analysis of the loss of function of DA and Hp-DRD1 was performed using *S*-(–)-carbidopa (carbidopa), which is an inhibitor of aromatic-L-amino acid decarboxylase, and morpholino antisense oligonucleotides (MASO) directed against *Hp-DRD1*.

MATERIALS AND METHODS

Incubation of gametes and zygotes

Sea urchins, *Hemicentrotus pulcherrimus* A. Agassiz, were collected in the vicinity of the Research Center for Marine Biology, Tohoku University, Japan. Gametes were obtained by intracoelomic injection of 0.5 mol l^{-1} KCl. Eggs were inseminated and incubated in filtered seawater (FSW) on a gyratory shaker in an incubator at 18°C until the appropriate developmental stages were reached.

Generation of anti-Hp-DRD1 antiserum and immunospecificity

A DNA sequence that encoded the hydrophilic C-terminal region of Hp-DRD1, namely R^{314}SFRNAFKTILFCYKCRGLSMRQA-DSSDDHTAMSNTSRQERLRGRLGNGYNTTPRPSHSDHRSSI-ENSAEQNQKMVKDTSLVIANKNANANVQDSKKDSSSPVA-VATITHSDA^{426}, was inserted into the vector pGEX-KG (Amersham Biosciences, GE Healthcare UK Ltd, Little Chalfont, UK) and the construct transformed into *Escherichia coli* BL-21 cells. The resulting glutathione S-transferase (GST)-fusion protein was purified from the supernatant obtained after sonication using a glutathione agarose column (Sigma-Aldrich Japan, Tokyo, Japan), and eluted with 10 mmol l^{-1} glutathione. The protein was concentrated by dialysis and used to inoculate rabbits with Freund's complete adjuvant (Difco Laboratories, Detroit, MI, USA). The immunospecificity of the antiserum was examined using whole-mount immunohistochemistry with or without 1.3 mg ml^{-1} GST-fusion protein in the primary antiserum.

Whole-mount immunohistochemistry

Embryos and larvae were fixed with 4% paraformaldehyde dissolved in FSW at the 5 hpf morula, 8 hpf unhatched non-rotatory blastula, 9.5 hpf unhatched rotatory blastula, 15 hpf swimming blastula, 20 hpf early gastrula, 24–29 hpf prism, 48 hpf two-arm pluteus, 67–68 hpf two-arm pluteus, and 34 days post-fertilization (dpf) eight-arm pluteus stages. To remove the fertilization envelope to ensure access of the antibody to unhatched blastulae, eggs were pretreated with 1 mmol l^{-1} amino triazole for 10 min before insemination (Showman and Froeder, 1979). After insemination, the softened fertilization envelopes were removed by passing the eggs through a 62 μm nylon mesh (Kyoshin Ricoh Inc., Tokyo, Japan). The fertilized eggs were incubated in a 6 cm diameter culture dish in an 18°C incubator without shaking until they reached the 8 hpf blastula or 9.5 hpf unhatched rotatory blastula stages. After fixation they were dehydrated in a series of increasing ethanol concentrations, and stored in 70% ethanol at 4°C until use.

Prior to antibody treatment, embryos were hydrated in phosphate-buffered saline with 0.1% Tween-20 (PBST), and then incubated for 24–48 h at 4°C with rabbit antibodies against DA (catalog number DA-1140, BIOMOL International LP, Plymouth Meeting, PA, USA or catalog number DOP11-S, Alpha Diagnostic International, San Antonio, TX, USA; diluted 1:150, the latter antibody was used only as an alternative to the DA-1140 antibody as stated in the text), rabbit antibodies against serotonin (Sigma-Aldrich Japan; 1:500), monoclonal antibody against γ-tubulin (EXBIO Praha, a.s. Vestec, Czech Republic; 1:1000), monoclonal antibody against acetylated α-tubulin (Sigma-Aldrich Japan; 1:500), rabbit antibodies against 5′-bromo-2′-deoxyuridine (BrdU; Sigma-Aldrich Japan; 1:250), monoclonal antibody Epith-2 against sea urchin epithelium plasma membrane (Kanoh et al., 2001), monoclonal antibody 1E11 against synaptotagmin, rabbit anti-Hp-DRD1 antiserum (1:500), or mouse antibodies against serotonin receptor (5HThpr) (Katow et al., 2004) (1:500), either diluted in PBST or undiluted in the case of the monoclonal antibodies. Anti-BrdU antibodies were applied after 1 h of treatment with 2 mol l^{-1} HCl to reveal incorporated BrdU. Anti-DRD1 antibodies were applied after treatment with 0.2% Triton X-100 for 2 min. After staining with the primary antibodies, the samples were washed with PBST three times (10 min each), and treated with Alexa Fluor 488- or 568-tagged anti-rabbit IgG or anti-mouse IgG antibodies (Invitrogen, Paisley, UK) for 2 h at ambient temperature. Samples were then washed with PBST three times (10 min each). The immunospecificity of the anti-DA antibody was tested using a mixture of the antibody (diluted 1:250 in PBST) and 200 μg ml^{-1} DA (Sigma-Aldrich), L-DOPA (L-3,4-dihydroxyphenylalanine; Sigma-Aldrich) or noradrenaline (norepinephrine) (Sigma-Aldrich). L-DOPA and noradrenaline exhibited no immunohistochemical reaction with the antibody. For double-immunohistochemistry, two of the above primary antibodies were applied consecutively in the order indicated in the text. To stain the DNA, 1 μmol l^{-1} propidium iodide (PI; SERVA Electrophoresis GmbH, Heidelberg, Germany) was applied during a PBST wash after incubation with the secondary antibody. The samples were examined under a Micro-Radiance confocal laser scanning microscope (Bio-Rad Microscience, Hemel Hempstead, UK) at the appropriate optical sections indicated in the text. Images were analyzed with NIH ImageJ software.

Bioassay of embryos treated with carbidopa

The aromatic-L-amino acid decarboxylase (AADC) inhibitor (2*S*)-3-(3,4-dihydroxyphenyl)-2-hydrazino-2-methylpropanoic acid [*S*-(–)-carbidopa, carbidopa; Sigma-Aldrich Japan] was applied either from soon after insemination until the 20 hpf early gastrula stage (before the appearance of the 5HT-NS) or from the 24 hpf prism larva stage until the 48 hpf pluteus stage (after the appearance of the 5HT-NS). The swimming activity of larvae that had been incubated with 4 ml of 0, 10, 15, 20 or 25 μmol l^{-1} carbidopa in FSW from the 24 hpf prism larva stage was assayed at 18°C for 2 h in 5 ml plastic bioassay tubes of 1.1 cm diameter, 7.5 cm height, and were mounted perpendicularly on a tube stand. The time period was set so that larvae could re-establish a stable vertical swimming pattern from initial tabulations due to the transfer of the suspension medium to the bioassay tubes but not progress to alter the stage of development. Firstly, 400 μl of larval suspension at the bottom of the tube was collected gently with a Pasteur pipette (bottom fraction). The remaining 3.6 ml of the larval suspension was then collected (vertical swimming fraction). The number of larvae in the bottom and the vertical swimming fractions was counted under a

dissection microscope. Each experiment was repeated three to four times using three to four different females with a total of 3512 embryos as controls, and 868, 821, 720 and 3999 embryos for the 10, 15, 20 and 25 μmol l^{-1} carbidopa treatments, respectively. The embryos that were treated with or without 25 μmol l^{-1} carbidopa soon after insemination were incubated in 4 ml of FSW in 5 ml plastic tubes and their swimming activity was examined as described above. Each experiment was repeated four times using four different females, and 2740 embryos were used as controls and 2602 embryos for the 25 μmol l^{-1} carbidopa treatment. The above results were analyzed by a paired two-tailed *t*-test using GraphPad Software QuickCalcs Online Calculators for Scientists (http://www.graphpad.com/quickcalcs/ttest1.cfm). Significance was set at $P<0.05$. DA rescue was carried out in the presence of 25 or 50 μmol l^{-1} of DA (Sigma-Aldrich Japan) in 25 μmol l^{-1} carbidopa. Oxidation of DA in sea water was prevented by adding anti-oxidant, 50 μmol l^{-1} of L(+)-ascorbic acid (Braubach et al., 2006). Each experiment was repeated three times using three different females, and a total of 1106 embryos were used for controls, 1176 embryos for the 25 μmol l^{-1} carbidopa treatment, 2912 embryos for treatment with a mixture of 25 μmol l^{-1} carbidopa and 25 μmol l^{-1} DA, and 4704 embryos for treatment with a mixture of 25 μmol l^{-1} carbidopa and 50 μmol l^{-1} DA. The above results were analyzed by a paired two-tailed *t*-test as stated above. An aliquot of embryos treated with a mixture of 25 μmol l^{-1} carbidopa and 25 μmol l^{-1} DA was examined with whole-mount immunohistochemistry for DA as stated above.

Reverse transcriptase polymerase chain reaction (RT-PCR)

Expression of *Hp-DRD1* mRNA was examined using 1 μg of cDNA template prepared from total RNA extracted from unfertilized eggs, fertilized eggs, 6 hpf morulae, 14 hpf swimming and 16 hpf mesenchyme blastulae, 20 hpf early gastrulae, 26 hpf prism larvae, and 48 hpf and 72 hpf two-arm plutei by PCR. The following primers were used: forward AACAAACGGAACAGACGAAGG; reverse GGACATCGATTGCGTTTCCAT, with an annealing temperature of 70°C (for the samples from unfertilized eggs, an annealing temperature of 60°C was used) for 30 cycles. Amplimers were purified with the Wizard SV Gel and PCR Clean-up System (Promega, Madison, WI, USA) and ligated into the vector pBluescript II (Stratagene, La Jolla, CA, USA). Clones were sequenced using a BigDye Terminator Cycle Sequencing Kit and an ABI PRISM 310 DNA Genetic Analyzer (PE Applied Biosystems, Tokyo, Japan), and found to encode a 1.3 kbp fragment of *Hp-DRD1* DNA delimited by the forward and reverse primers (data not shown). Potential contamination with genomic DNA was analyzed by performing PCR without the addition of reverse transcriptase at each developmental stage. For the positive control, the *ubiquitin* gene from *H. pulcherrimus* (*Hp-ubi*) was amplified from 1 μg of *H. pulcherrimus* cDNA using the following primers: forward DGAGCTGCHATGTATTTGCCAGAYG; reverse TTTGATGGAATAACAAATAACYGATTGCTT.

MASO injections

Unfertilized eggs were attached to plastic dishes coated with 1% protamine sulfate, inseminated, and microinjected with a 1% egg volume of 500 μmol l^{-1} or 750 μmol l^{-1} *Hp-DRD1*-MASO (CCGTTTGTTAAATTATTCGTCATGG) or 750 μmol l^{-1} standard control MASO (Gene Tools, LLC, Philomath, OR, USA). A total of 745 eggs from three different females were used in experiments performed in triplicate. The injected eggs were incubated overnight at 18°C until they hatched, and then transferred to fresh FSW in plastic dishes until the 20 hpf early gastrula stage. At 20 hpf they were transferred to fresh FSW in 1.5 ml polystyrene disposable micro-cuvettes for spectroscopy (10 mm wide, 4 mm deep, 45 mm high; Kartell, Milan, Italy), and incubated for 2 h at 18°C. Firstly, 200 μl of embryo suspension were collected gently from the bottom of the cuvette using a Pasteur pipette, and then the remaining suspension in the cuvettes was collected. These embryos were counted under a dissection microscope. The total number of embryos examined for the bioassay was 186 controls, 201 for the 500 μmol l^{-1} MASO treatment, and 177 for the 750 μmol l^{-1} MASO treatment. The results obtained were analyzed by a paired two-tailed *t*-test using GraphPad Software QuickCalcs Online Calculators for Scientists. Significance was set at $P<0.05$.

The remaining 181 embryos from the total of 745 were fixed with 4% paraformaldehyde and the expression of Hp-DRD1 and DA was examined with appropriate antibodies under a confocal laser scanning microscope as stated above. To quantify the influence of *Hp-DRD1*-MASO injection, the number of dopaminergic granules (DAGs) was counted in four control MASO-injected embryos and seven *Hp-DRD1* MASO-injected ones. Another 11 control MASO-injected embryos and nine *Hp-DRD1*-MASO-injected ones were used for counting the number of DRD1 granules. The laser beam-excited positive signals of DA and DRD1 were clear only on the side of the embryo that was closer to the laser discharge device. Thus, the number of DAGs or DRD1 granules that was counted on this side represented one-half of an embryo (half number of positive granules, HNPGs). These calculations were statistically analyzed by a paired two-tailed *t*-test using GraphPad Software QuickCalcs Online Calculators for Scientists. Significance was set at $P<0.05$.

RESULTS

Formation of DAGs

DA was not detected before the exhibition of rotatory movement by embryos in the fertilization envelope at the 8 hpf blastula stage (Fig. 1A). At the 9.5 hpf rotatory blastula stage, immediately before they hatched, DA was detected in association with 1 μm diameter DAGs present throughout the apical surface of the ectoderm (Fig. 1B), with DAGs detected on embryonic and larval surfaces until metamorphosis (Fig. 1C–K). DAGs were not detected when the anti-DA antibody was pre-absorbed with DA (DA-absorbed antibody, Fig. 1F), and the anti-DA antibody did not cross-react with L-DOPA or noradrenaline (data not shown). At the 48 hpf pluteus stage, the number of DAGs increased significantly, and formed a broad band around the circumoral ciliary band region (Fig. 1G). The DAGs at the circumoral ciliary band region converged to become a distinctive sharp-edged circumoral stripe (DAG stripe) by the 67 hpf pluteus stage (Fig. 1H). By the 34 dpf eight-arm pluteus stage, the DAGs converged to a narrower stripe at each of the eight arms and at the anterior and posterior epaulets (Fig. 1I). These stripes did not react with the DA-absorbed antibody (Fig. 1J). However, the signal in the middle of the larval arms and posterior area of the larval body was non-specific, because pre-absorbed antibody bound to these areas (Fig. 1J, arrowheads). The DAG stripe at the epaulets remained throughout metamorphosis (Fig. 1K), and the pattern of DAG expression resembled the pattern of distribution of cilia on the surface of embryos and larvae. The pad of the primary podia of the adult rudiment expressed DA (Fig. 1K, small arrows). During metamorphosis, absorption of the dorsal (ab-anal) ectoderm by the adult rudiment occurred earlier (Fig. 1K, ab-anal) than that of the ventral (anal) ectoderm (Fig. 1K, anal). The DAGs were also seen in 24 hpf prism larvae (Fig. 1L) and 68 hpf plutei (Fig. 1M) that were stained with the alternative rabbit anti-DA antibody (DOP11-S). The

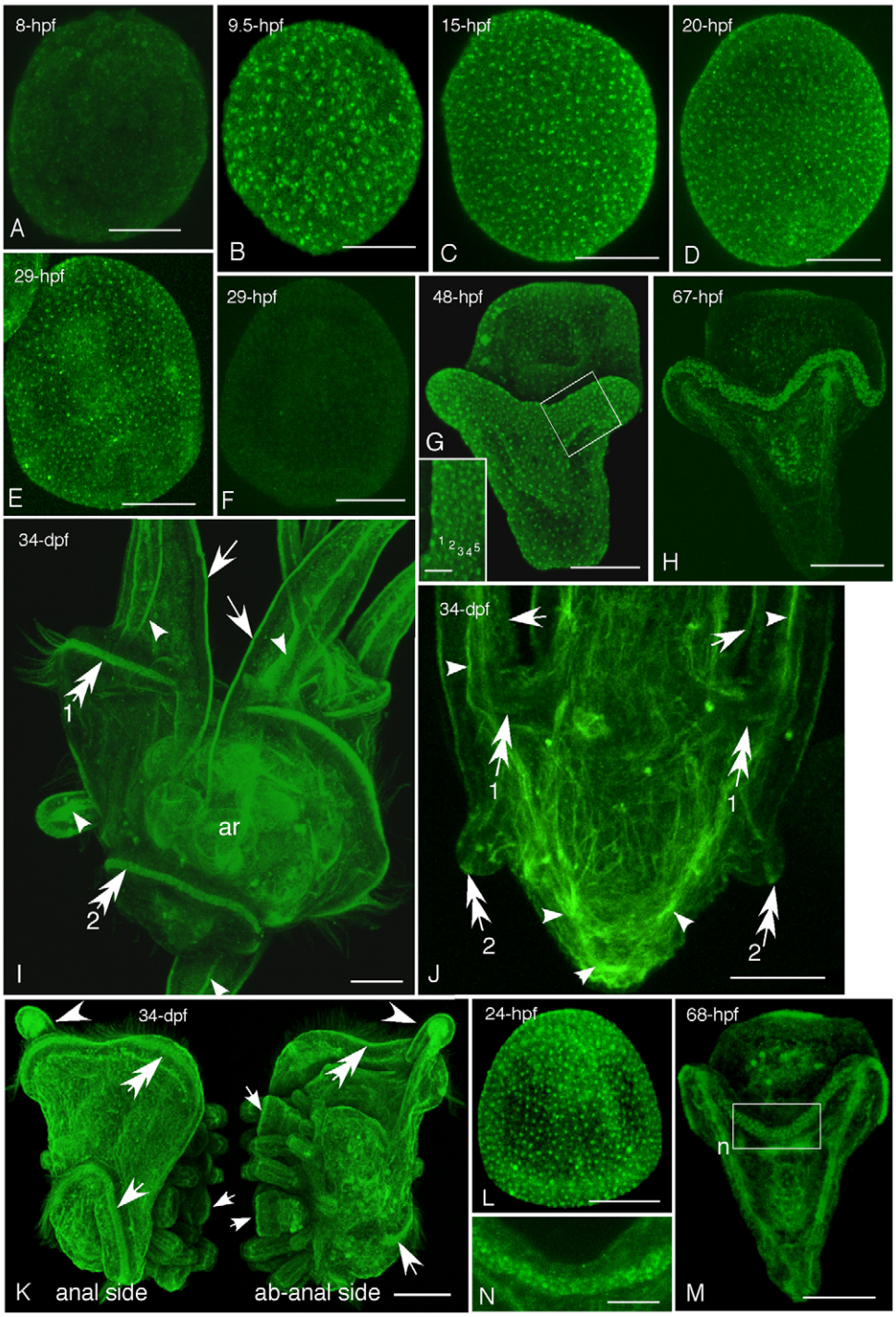

Fig. 1. Immunohistochemistry of dopaminergic granules (DAGs) using anti-dopamine (DA) antibody. (A) An 8 h post-fertilization (hpf) unhatched non-rotatory blastula. (B) A 9.5 hpf unhatched rotatory blastula. (C) A 15 hpf swimming blastula. (D) A 20 hpf early gastrula. (E) A 29 hpf mid-gastrula. (F) Immunohistochemistry performed on a 29 hpf mid-gastrula using DA-absorbed anti-DA antibody. (G) A 48 hpf pluteus. Inset, high magnification of the five-row striped pattern shown in the rectangle. Numbers 1–5 indicate rows of DAGs. (H) A 67 hpf pluteus. (I) Left-side view of a 34 dpf (days post-fertilization) eight-arm pluteus. Arrows indicate the ciliary band of the larval arms. Arrowheads indicate non-specific binding of the primary antibody. Double-arrows 1 and 2 indicate anterior and posterior epaulets, respectively. ar, adult rudiment. (J) Posterior half of a 34 hpf 8-arm pluteus incubated with DA-absorbed antibody. Anterior (double-arrow 1) and posterior epaulets (double-arrow 2) and the ciliary band region of a larval arm (arrows) did not bind to the secondary antibody. Arrowheads indicate non-specific binding of the antibody. (K) Montage of a pluteus during metamorphosis viewed from the ventral (anal) and dorsal (ab-anal) sides taken by flipping a sample under the microscope. Arrowheads indicate the remains of an arm. Arrows and double-arrows indicate the posterior and anterior epaulets, respectively. Small arrows indicate the DA-positive tip of the pad. (L) A 24 hpf prism larva incubated with the alternative anti-DA antibody. (M) A 68 hpf pluteus incubated with the alternative anti-DA antibody. (N) High magnification of the ciliary band shown in the rectangle (labeled n) in M. Scale bars: A–J, 50 μm; L and M, 20 μm; G inset, 15 μm; N and K, 100 μm.

antibody also recognized DAGs in the ciliary band of 68 hpf plutei (Fig. 1N), indicating that the DAGs were recognized by two antibodies. This excluded the possibility of immunoreaction by antibodies from a particular manufacturer.

To examine how closely the pattern of distribution of the DAG stripes resembled that of the cilia, the cytological localization of the DAGs was examined by immunostaining with anti-DA antibody and an Epith-2 monoclonal antibody, which is specific to the lateral plasma membrane of epithelial cells (Kanoh et al., 2001). This staining revealed that each DAG was positioned apically (Fig. 2A, inset) in the middle of a single ectodermal cell (Fig. 2A).

The sub-cellular localization of DAGs was analyzed further by immunostaining with anti-DA antibody and anti-γ-tubulin antibody as a marker of the basal body of the cilium (Muresan et al., 1993; Hagiwara et al., 2000). These antibodies were co-localized at the apical side of the ectoderm. Anti-γ-tubulin antibody was associated with granules of approximately 0.7 μm in diameter (Fig. 2B). Staining of serial 0.5 μm optical sections revealed granules near the apical surface of the ectoderm that stained positive for both antibodies (Fig. 2C0), which were replaced (Fig. 2C0.5–1.5) by staining for γ-tubulin alone 2 μm from the surface (Fig. 2C2). These findings suggest that DAGs are located on the apical side of γ-

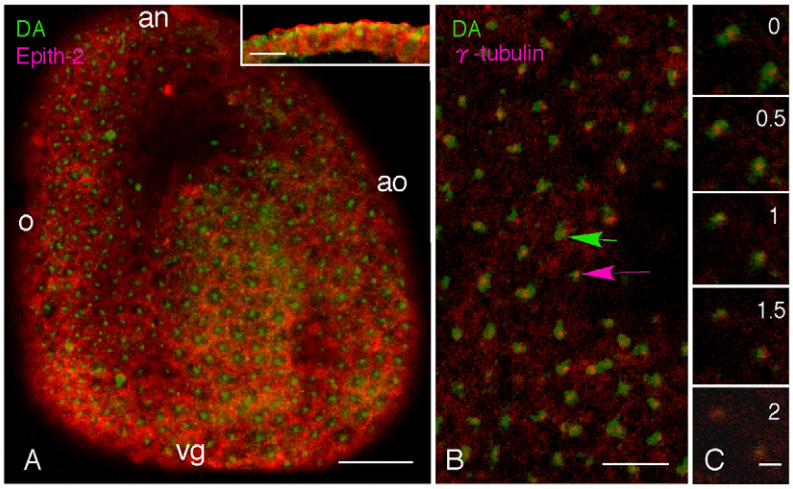

Fig. 2. Immunohistochemical distribution pattern of DAGs in a 24 hpf prism larva. (A) Double-immunostaining for dopamine (DA, green) and Epith-2 (plasma membrane, red). an, animal pole; ao, aboral side; o, oral side; vg, vegetal pole. Inset: sagittal view of the larval ectoderm showing the apical localization of DA granules (green and yellow dots). (B) Double-immunostaining of DA (green) and γ-tubulin (red). Green arrow, DA; magenta arrow, γ-tubulin. (C) Serial 0.5 μm-thick optical sections of the apical ectoderm from 0 to 2 μm deep toward the basal side. DA (green) is localized at the apical side of γ-tubulin (red), with some overlap. Scale bars: A, 30 μm; A inset, 10 μm; B, 10 μm; C, 2 μm.

tubulin, and therefore are associated with the basal bodies of ectodermal cilia.

The above spatial relationship was tested in 34 dpf plutei by double-immunostaining for DA (Fig. 3A,D,G; DA) and acetylated-α-tubulin (Fig. 3B,E,H; AT). Unlike γ-tubulin, acetylated α-tubulin is a component of various microtubules, which include those located in cilia (Steffen et al., 1994). Accordingly, the anti-acetylated-α-tubulin antibody stained microtubules in the larval ectoderm (Fig. 3B, arrows), cilia at the ciliary bands above the mouth (Fig. 3B rectangle e, Fig. 3E), and epaulets (Fig. 3B rectangle h, Fig. 3H). The merged image indicated clearly that DAGs were localized at the base of each cilium (Fig. 3C,F,I; DA/AT), which suggested that there may be a structural basis for the involvement of DA in ciliary beating, and thus in the swimming activity of embryos and larvae.

The swimming activity of larvae is regulated by the 5HT-NS (Yaguchi and Katow, 2003; Katow et al., 2007). Given that the larval 5HT-NS expresses synaptotagmin (anti-synaptotagmin antibody-positive nervous system, Syn-NS) (Katow et al., 2009), the distribution of the 5HT-NS in larvae was examined using an anti-synaptotagmin antibody. The spatial distribution patterns of the Syn-NS and DAGs were examined in 34 dpf plutei by immunohistochemistry, which revealed that the Syn-NS and DAGs showed distinctly separate patterns of distribution (Fig. 4A–C). In the larval arms, DAGs were aligned parallel to the apical surface of the ectoderm. They were separate from the Syn-NS fibers, but were associated closely with regularly arranged perpendicular Syn-NS fibers (Fig. 4D, arrowheads), which suggested that the DAG stripe was not connected structurally to the Syn-NS. The DAG

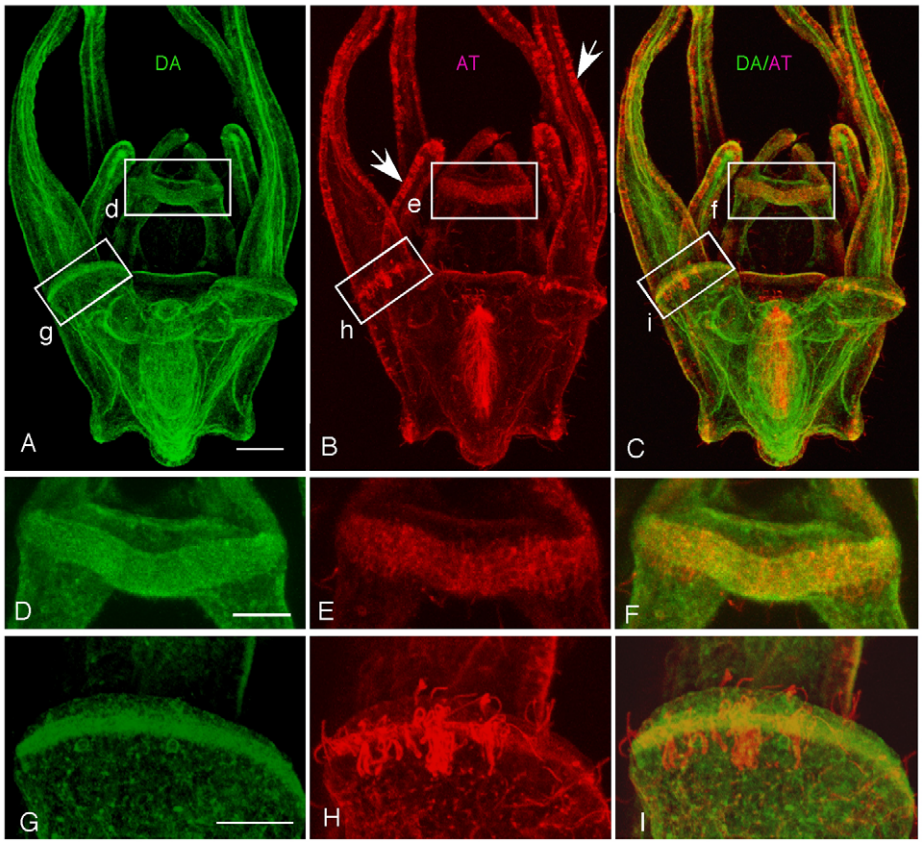

Fig. 3. Immunohistochemistry of 34 dpf eight-arm pluteus that illustrates the spatial relationship between the DAG stripes (green) and acetylated α-tubulin (red). Low-magnification images of DAG stripes (A, DA), acetylated α-tubulin (B, AT) and a merged image (C, DA/AT). (D–F) Higher-magnification images of a ciliary band at the upper lip region shown in rectangles d–f in A–C. (G–I) Higher-magnification images of the right anterior epaulet shown in rectangles g–i in A–C. Scale bars: A, 100 μm; D and G, 20 μm.

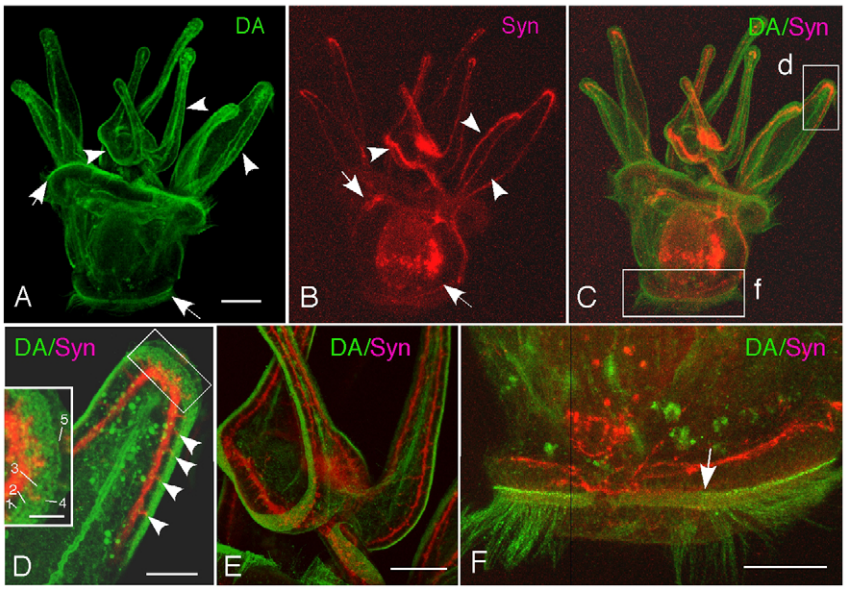

Fig. 4. Immunohistochemistry of 34 dpf eight-arm plutei illustrating the spatial relationship between the DAG stripes (DAG; DA, green) and the synaptotagmin-expressing nervous system (Syn-NS; Syn, red). (A) DAG stripes were present on the larval arms (arrowheads) and epaulets (arrows). (B) Syn-NS. Arrows and arrowheads indicate epaulets and larval arms, respectively. (C) Merged image of A and B showing that the DAGs and Syn-NS did not colocalize. (D) Higher-magnification image of DAG stripes on the pluteus arm indicated with a rectangle (labeled d) in C. Arrowheads show periodical spikes of Syn-NS. Inset shows higher-magnification image of the five-row pattern of DAG stripes (numbers 1–5) shown by the rectangle. (E) DAG stripes on the basal region of the larval arms showing structural continuation of these stripes without co-localization with the Syn-NS. (F) DAG stripes at the posterior epaulet indicated with a rectangle (labeled f) in C were separate from the Syn-NS. A minor Syn-NS fiber was associated closely with the anterior edge of a DAG stripe (arrow). Scale bars: A, 100 μm; D–F, 50 μm; D, inset, 25 μm.

stripes continued along the larval arms (Fig. 4E). Although the primary Syn-NS branch was aligned parallel to the DAG stripe, with a space between the most anterior edge of the DAG stripe at the epaulets, the minor Syn-NS fibers were localized closer to the DAG stripe (Fig. 4F, arrow).

DA/DRD1 granule formation

To examine the changes over time of the expression of the DA receptor, the expression patterns of both the *Hp-DRD1* mRNA and the associated protein were examined. Analysis by RT-PCR showed that the *Hp-DRD1* transcript was present in unfertilized eggs (Fig. 5A, lane 1) and that its relative concentration was significantly lower in fertilized eggs (Fig. 5A, lane 2). However, the transcript was then detected continuously and clearly from the 6 hpf morula stage (Fig. 5A, lane 3) to the 72 hpf pluteus stage (Fig. 5A, lane 9).

Hp-DRD1 protein was not detected immunohistochemically in 8 hpf unhatched non-rotatory blastulae (Fig. 5B). However, by the time the embryos had acquired rotatory movement in the fertilization envelope, before hatching at 9.5 hpf, DRD1 granules were expressed on the embryonic surface in an irregular pattern (Fig. 5C). After the 20 hpf early gastrula stage, the size of the DRD1 granules decreased, and the granules were arranged throughout the embryonic surface (Fig. 5D). Immunofluorescence was not detected when the antibody was pre-absorbed with the Hp-DRD1-GST-fusion protein (Fig. 5E), which indicated that the positive immunoreaction was specific to Hp-DRD1. The distribution pattern was remarkably similar to that of the DAGs (Fig. 1). Like the DAGs, the DRD1 granules converged at the circumoral ectodermal region by the 48 hpf pluteus stage (Fig. 5F). The DRD1 granules were localized in stripes on the larval arms and epaulets by the 34 dpf pluteus stage (Fig. 5G, arrows and double-arrows, respectively, inset labeled a). These DRD1 granules were aligned in five rows of stripes (Fig. 5G, inset labeled b), which were reminiscent of the five-row striped pattern of DAGs seen in the larval arms (Fig. 4D, inset, numbers 1–5). Each of these DRD1 granules overlapped partially with γ-tubulin on the apical side (Fig. 6A–C). DRD1 granules were located at the apical side of the cell (Fig. 6D), and overlapped with γ-tubulin 2.9 μm below the cell surface (Fig. 6E). At 4 μm from the apical surface, only γ-tubulin was observed to be present (Fig. 6F). Although the distances of the DRD1 granules and γ-tubulin from the apical surface of the cell of 34 dpf larval arms were not the same as those of DAGs and γ-tubulin in 24 hpf prism larvae (Fig. 2), the DRD1 granules and DAGs were located very close to γ-tubulin, which suggests that DAGs and DRD1 granules are strongly co-localized at the base of the cilium. The exact relationship between DAGs and DRD1 granules was not examined by immunohistochemical double-staining owing to the fact that the Triton X-100 treatment necessary for the Hp-DRD1 immunohistochemistry results in the loss of the antigenicity of DA.

Spatial relationship between the serotonin receptor cell network, Hp-DRD-1 stripes and the 5HT-NS in larvae

Immunostaining of DA and synaptotagmin (Fig. 4) suggested the existence of an interaction between the Hp-DRD1 stripes and the 5HT-NS. This could provide the morphological basis of the swimming activity of larvae involving both the 5HT-NS and the DA/Hp-DRD1 system. In 34 dpf eight-arm plutei, an Hp-DRD1 stripe at the anterior and at the posterior epaulet was located between two major branches of the serotonin receptor cell network (SRCN) (Fig. 7A–D for anterior epaulet). Its anterior edge was close to a minor branch of the SRCN (Fig. 7C,D, arrow), whereas two major branches were distinctly separate from the Hp-DRD1 stripe. The SRCN, on the other hand, had a pattern similar to that of the 5HT-NS (Fig. 7E–H). In particular, the SRCN, 5HT-NS (Fig. 7H) and Hp-DRD1 stripes (Fig. 5G) exhibited highly similar patterns at the base of the larval arms. At the epaulet region, these three components exhibited patterns similar to those observed at the base of the larval arms (Fig. 7I).

Convergence of DA/DRD1 granules on the ciliary bands

The dynamic reorganization of the pattern of DA/DRD1 granule (DA/DRD1-G) distribution on the larval surface that was observed during formation of the ciliary band was initiated at around the 48 hpf pluteus stage (Fig. 1G, Fig. 5F). This implicates several morphogenetic mechanisms, such as local changes in cell shape associated with convolution of the ectodermal cell sheet and/or local proliferation of ectodermal cells, in this process.

To examine possible changes in cell shape, the ciliary bands of the larval arms were analyzed by immunostaining with anti-Hp-DRD1 antiserum and Epith-2 (Fig. 8A–C). The Epith-2 staining pattern indicated that the region contained a larger number of smaller

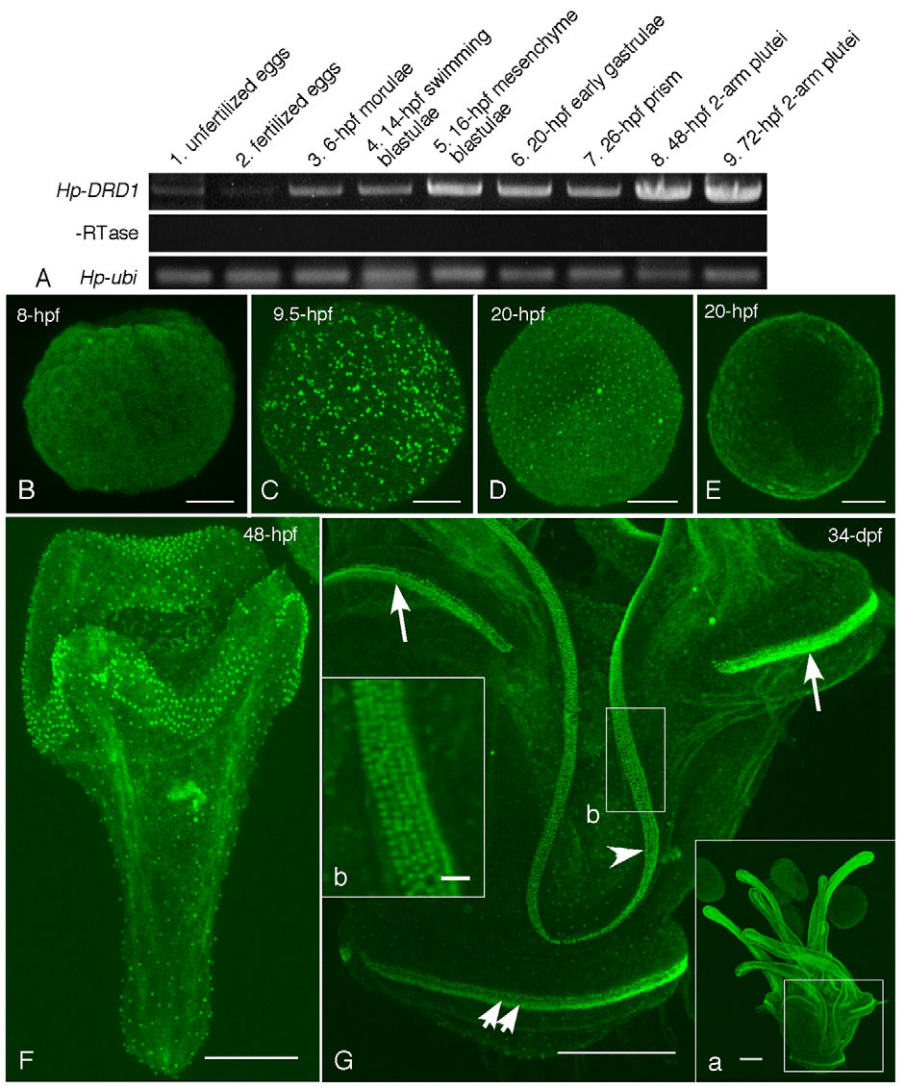

Fig. 5. Expression pattern of Hp-DRD1.
(A) Changes in the pattern of accumulation of *Hp-DRD1* mRNA over time were evaluated by RT-PCR (top row). Lane 1, unfertilized eggs; lane 2, fertilized eggs; lane 3, 6 hpf morulae; lane 4, 14 hpf swimming blastulae; lane 5, 16 hpf mesenchyme blastulae; lane 6, 20 hpf early gastrulae; lane 7, 26 hpf prism larvae; lane 8, 48 hpf two-arm plutei; and lane 9, 72 hpf two-arm plutei. The middle row shows the control PCR results with no reverse transcriptase. The bottom row shows the results obtained with the *Hp-ubiquitin* primers (positive control).
(B–G) Immunohistochemistry of Hp-DRD1 expression. (B) An 8 hpf unhatched non-rotatory blastula. (C) A 9.5 hpf unhatched blastula at the acquisition of rotatory movement expressing Hp-DRD1 in association with granules. (D) A 20 hpf early gastrula. (E) A 20 hpf early gastrula in which the antibody had been pre-absorbed with Hp-DRD1-GST-fusion protein. (F) A 48 hpf pluteus. The DRD1 granules were densely packed in the circumoral ectodermal region, whereas they were sparsely distributed in the posterior body region. (G) DRD1 granules were concentrated at the major ciliary bands on the arms (arrowhead) and anterior (arrows) and posterior epaulets (double-arrows) of the 34 dpf eight-arm pluteus. Inset labeled a shows the entire body of the larva at low magnification. The rectangle indicates the part of the larva shown in G. The DRD1 granules comprised a characteristic five-row striped pattern (rectangle labeled b and inset b) and, at the epaulets, the stripes were less distinctive. Scale bars: B–E, 30 μm; F and G inset a, 100 μm; G inset b, 5 μm; G, 80 μm.

cells (Fig. 8B, solid line rectangle) than was found in the non-ciliary band of ectoderm that surrounded the ciliary band (Fig. 8B, dashed-line rectangle). The merged image shows a single DA/DRD1-G per cell in the ciliary band (Fig. 8C, solid-line rectangle and inset). Thus, the possibility of the local appearance of cells with multiple DA/DRD1-Gs was ruled out. The cell number seemed too large for simple changes in cell shape, and seemed to suggest an increase in the number of cells that expressed DA/DRD1-G. The merged image also indicated that the non-ciliary band of ectoderm that surrounded the ciliary band did not express DA/DRD1-G (Fig. 8C, dashed-line rectangle). These observations suggest that local proliferation of cells and the loss of DA/DRD1-Gs from the ectodermal cells in the region adjacent to the ciliary band are responsible for the distribution pattern of DA/DRD1-Gs.

To examine the local proliferation of cells, plutei were incubated with 0.1 μmol l^{-1} BrdU for 7 h from either the 41 hpf to the 48 hpf stage or the 44 hpf to the 51 hpf stage. These are the periods during which the ciliary band emerges (Fig. 1H). In 48 hpf plutei, BrdU-positive cells comprised a broad circumoral band (Fig. 8D) in which nuclei also accumulated (Fig. 8E,F). In 51 hpf plutei, the circumoral band of BrdU-positive cells was narrower than that in younger plutei (Fig. 8G), and the nuclei accumulated in the circumoral region (Fig. 8H,I). These observations indicate that formation of the ciliary band is associated with: (1) local changes in the shape of ectodermal cells, (2) withdrawal of DA/DRD1-Gs from nearby ectodermal cells that are not part of the ciliary band, and (3) active proliferation of ectodermal cells at the ciliary band.

Role of DA/DRD1-Gs in swimming in embryos and larvae

The immunohistochemical studies described herein suggest that DA/DRD1-Gs are the morphological basis of a dopaminergic system that regulates swimming in embryos and larvae. In support of this, we found that synthesis of DA was inhibited by carbidopa, a potent inhibitor of AADC (Gilbert et al., 2000), in larvae that were treated from the 24 hpf prism stage, the stage when the 5HT-NS emerges, to the 48 hpf pluteus stage. The swimming activity of these larvae was not affected significantly at concentrations of carbidopa ≤15 μmol l^{-1}. However, upon treatment with 20–25 μmol l^{-1} carbidopa, the swimming activity decreased significantly in a dose-dependent manner (P<0.05; Fig. 9A). Larvae that had sunk to the bottom of the bioassay tubes showed spasmodic, weak movement.

In plutei treated with 25 μmol l^{-1} carbidopa, DAGs associated with the ciliary band were scarcely detected (Fig. 9B). Carbidopa also caused a dose-dependent delay or inhibition of morphogenesis in some cases, which resulted in features such as the slightly under-

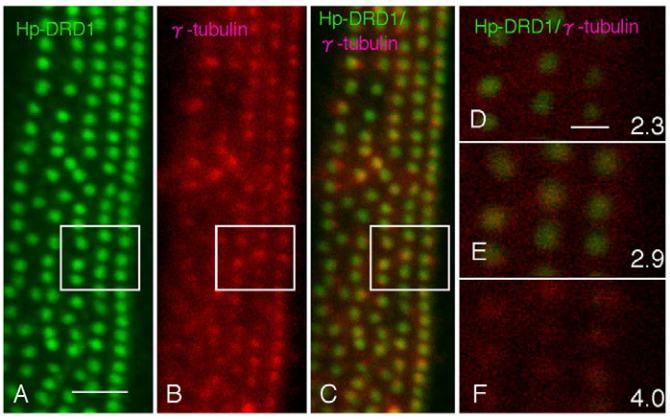

Fig. 6. Immunohistochemistry to demonstrate the five-row striped pattern of DRD1 granules at the ciliary band of a 34 dpf larval arm. (A) Five-row pattern of DRD1 granules. (B) Five-row pattern of γ-tubulin associated with 0.6 μm diameter granules in the same optical section as A. (C) Merged image of A and B showing perfect overlap between the images of the two proteins. (D) Higher magnification of the merged image of C for the area indicated by a rectangle and 2.3 μm from the apical surface of the ectoderm. Hp-DRD1 (green) was predominant. (E) At 2.9 μm from the cell surface, the two proteins were co-localized. (F) At 4 μm from the cell surface, γ-tubulin (red) alone was detected. Scale bars: A, 5 μm; D, 2 μm.

developed larval arms (Fig. 9B). Carbidopa was lethal at a concentration of 50 μmol l^{-1} (data not shown).

The target enzyme of carbidopa is also involved in the synthesis of serotonin. Thus, it was possible that the effect of carbidopa on larval swimming was not due to effects on DA but was instead due to the inhibition of serotonin synthesis. However, immunohistochemical analysis indicated clearly that the 5HT-NS was not affected visibly by carbidopa even at a concentration of 25 μmol l^{-1} (Fig. 9C,D), and therefore the reduced level of swimming by larvae could not have been due to a decreased level of serotonin synthesis or morphogenetic delay, but rather to the perturbation of DA synthesis.

The 5HT-NS of the larvae of sea urchins has long been regarded as the primary apparatus that regulates the beating of cilia during larval swimming (Yaguchi and Katow, 2003; Katow et al., 2004; Katow et al., 2007). However, the mechanisms that underlie the period of serotonin-independent swimming that occurs from soon after hatching until immediately before serotonergic ganglion development at the 24 hpf prism larva stage have been an ongoing mystery (Yaguchi and Katow, 2003). In the present study, we detected DA/DRD1-Gs at 9.5 h before hatching, which is close to the time when the blastulae acquire rotatory movement in the fertilization envelope (Fig. 1B). This strongly suggests that the DA/DRD1-G system could be an important contributor to ciliary beating in early embryos.

Embryos treated with 25 μmol l^{-1} carbidopa soon after insemination developed normally until the 15 hpf swimming blastula stage and had apparently normal swimming activity. However, a few hours later, at the 20 hpf early gastrula stage, their swimming activity decreased rapidly, and 90% of them had sunk to the bottom of the bioassay tubes (Fig. 10A), and showed weak spasmodic movement. Expression of DAGs in these embryos was found to have decreased considerably (Fig. 10B,C), whereas DRD1 granules were not affected (Fig. 10D,E). Longer periods of incubation with carbidopa resulted in the death of most embryos. The effects of this reagent were considerably more severe in early embryos than in 24 hpf prism larvae (Fig. 9A). However, in the presence of exogenous DA, the swimming activity was restored in a dose-dependent manner; $P<0.05$ between control and 25 μmol l^{-1} DA, and $P>0.05$ between control and 50 μmol l^{-1} DA. Expression of DA granules was considerably restored in the embryos that were treated with a

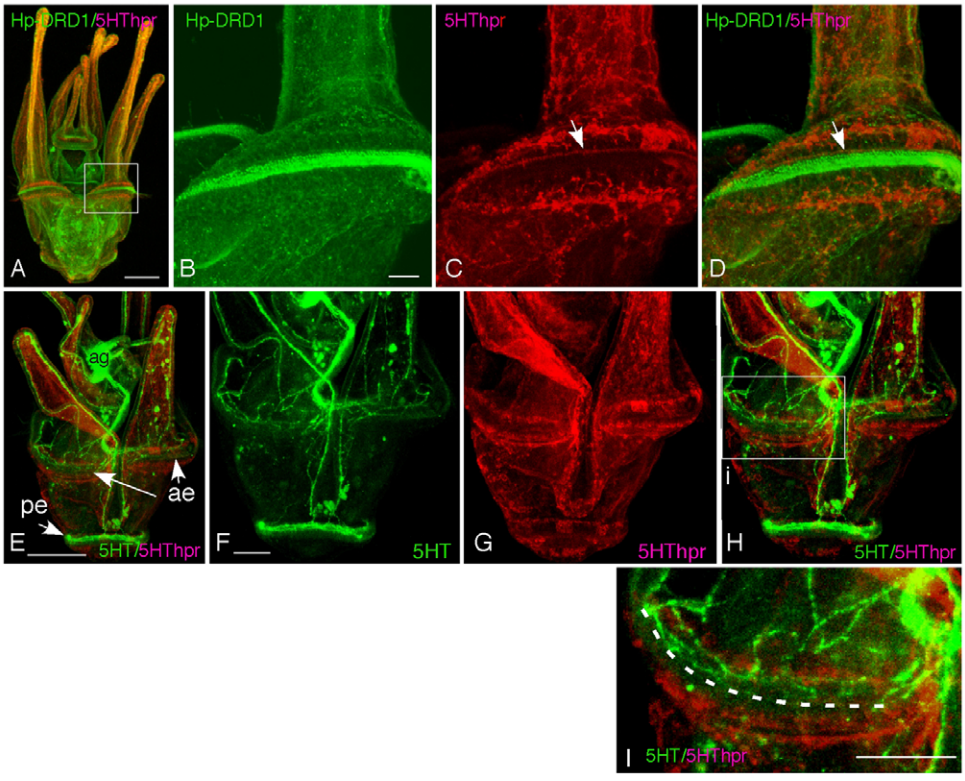

Fig. 7. Immunohistochemistry of 34 dpf eight-arm pluteus larvae showing the topological relationship between Hp-DRD1 and the serotonin receptor cell network (SRCN; 5HThpr) (A–D), and serotonergic cells and the SRCN (E–I). (A) Low-magnification image shows the whole-body distribution of Hp-DRD1 (green) and serotonin receptor cells (5HThpr, red). (B) Higher-magnification image of the anterior epaulet (rectangle shown in A) stained with Hp-DRD1. (C) Same region as shown in B stained for 5HThpr. (D) Merged image of B and C showing the spatial relationship between Hp-DRD1 and 5HThpr. Arrows in C and D indicate a minor SRCN branch. (E) Low-magnification image showing the whole-body distribution of serotonergic cells (green) and SRCN (red). ae, anterior epaulet; ag, apical ganglion; pe, posterior epaulet. (F) High-magnification image of the posterior half of the body stained for serotonin. (G) Same region as in F stained for 5HThpr. (H) Merged image of F and G. (I) Higher-magnification image of anterior epaulet region indicated by rectangle labeled i in H. White dashed curve indicates approximate location of Hp-DRD1 stripe. Scale bars: A and E, 100 μm; B, 20 μm; F and I, 50 μm.

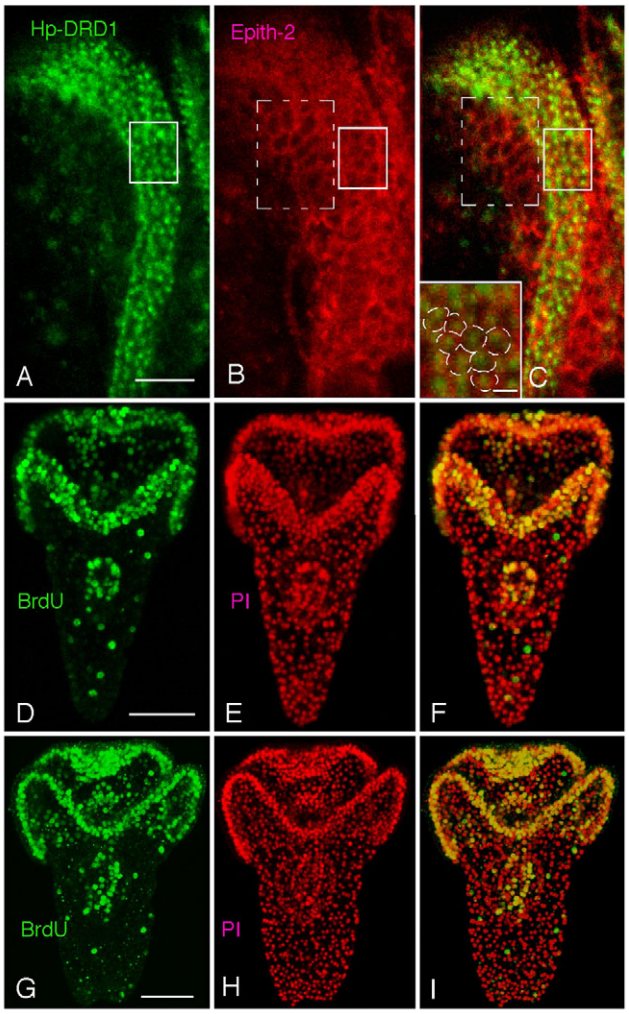

Fig. 8. Immunohistochemistry of the larval ciliary band region. (A–C) A 34 dpf pluteus immunostained for Hp-DRD1 (green) and the plasma membrane of ectodermal cells (Epith-2, red). (A) DRD1 granules. (B) Ectodermal cells. (C) Merged image of A and B showing a DRD1 granule in each ectodermal cell at the ciliary band, whereas the non-ciliary band ectoderm contains no DRD1 granules (dashed-line rectangle). The inset shows a higher-magnification image of the area indicated by the solid-line rectangle. The dashed line indicates the contours of cells stained for Epith-2. (D–I) Double-staining with anti-BrdU antibody (green) and PI nuclear stain (red). (D–F) Localized proliferation of ectodermal cells at the circumoral region in a 48 hpf pluteus. (D) A broad band of BrdU-positive nuclei. (E) PI-stained nuclei. (F) Merged image of D and E. (G–I) Accumulation of BrdU-positive nuclei at the ciliary band region of a 51 hpf pluteus. (G) A band of BrdU-positive nuclei narrower than that in D. (H) Nuclei with PI stain. (I) Merged image of G and H showing a stripe of BrdU-positive nuclei narrower than that in F at the ciliary band region. Scale bars: A, 10 μm; C inset, 2 μm; D and G, 50 μm.

mixture of 25 μmol l^{-1} carbidopa and 25 μmol l^{-1} DA (Fig. 10G), which indicated that the swimming activity and the formation of DA granules of early embryos are heavily dependent on DA.

To examine whether knockdown of the Hp-DRD1 protein affected the swimming activity of larvae, a MASO that was directed against *Hp-DRD1* was microinjected into eggs soon after fertilization. The eggs developed normally until around the 18 hpf swimming blastula stage. However, during the following 2–3 h, the swimming activity of the MASO-treated embryos decreased rapidly in a dose-dependent manner (Fig. 11A). In 20 hpf embryos injected with 750 μmol l^{-1} MASO, swimming activity decreased significantly (P<0.05), whereas only a small decrease was observed between the control and 500 μmol l^{-1} MASO groups. Expression of DRD1 granules was severely inhibited (Fig. 11B,C); HNPGs for DRD1 in *Hp-DRD1*-MASO-injected embryos was 77.6±22.8/embryo (N=9) and that of control MASO-injected embryos was 226.8±75.4/embryo (N=11) (P<0.005). However, formation of DAGs was virtually unaffected by MASO treatment (Fig. 11D,E); HNPGs for DA of control MASO-injected embryos was 400.3±94.6/embryo (N=4) and that in *Hp-DRD1*-MASO-injected embryos was 386±61.8/embryo (N=7) (P=0.9259). Taken together with the depletion of DAGs induced by carbidopa (Fig. 9B), the MASO results suggest that the formation of DAGs is independent of the formation of DRD1 granules.

DISCUSSION

Formation of DA/DRD1-G stripes and the ciliary band

The high concentration of DA/DRD1-Gs in the ciliary bands of larval arms and epaulets supports the notion that the dopaminergic system is involved in the regulation of the beating of cilia. This pattern of expression is remarkably similar to that identified in a previous whole-mount *in situ* hybridization study of the expression of *Hp-DRD1* mRNA (Suyemitsu, 2007). Convergence of DA/DRD1-Gs from the initial evenly distributed pattern in embryonic stages to the well-organized ciliary band pattern occurs at around the 48 hpf early pluteus stage. This is similar to the findings related to the pattern of ciliary band formation in the doliolaria larvae of *Florometra serratissima* that were obtained by scanning electron microscopy (Lacalli and West, 1986). Our immunohistochemical results suggest that the major driving mechanism of ciliary band formation includes the local proliferation of ectodermal cells and the loss of DA/DRD1-Gs from the cells around the ciliary band ectoderm. According to the *in situ* hybridization database of the Sea Urchin Genome Project (http://goblet.molgen.mpg.de/eugene/cgi/eugene.pl), several region-specific genes are transcribed in the ciliary band ectoderm, which includes genes related to cell proliferation such as *Sp-early histone H3*, a *histone H3* homolog (Kase et al., 2006); *Sp-Hes*, a *hes* homolog (Castella et al., 2000); and *Sp-PaxC*, a neurogenetic *paxC* homolog (Hadrys et al., 2005). These genes might provide the genetic basis for local cell proliferation during formation of the ciliary band, and will be an interesting focus of future study.

As mentioned above, the five-row striped pattern of DA/DRD1-Gs, which was typically seen in the ciliary band of the larval arm, emerged at the 48 hpf pluteus stage. The number of rows remained constant throughout larval development until immediately before metamorphosis at around the 34 dpf eight-arm pluteus stage. At this stage, the number of rows of DA/DRD1-Gs increased to approximately seven at the apical tuft region. The mechanism of formation of the rows of granules remains to be elucidated.

Morphological basis of the preneural dopaminergic system for the regulation of swimming

We have shown here that DA/DRD1-Gs are expressed at the same time as the acquisition of rotatory movement before hatching. Our previous observations indicated that embryonic swimming activity is insensitive to the absence of serotonin in embryos treated with *p*CPA (Yaguchi and Katow, 2003). These observations, together with those from a previous study (Soliman, 1983b), suggest that the swimming activity of early embryos is not regulated by the 5HT-NS. Formation of DAGs was inhibited by the suppression of DA synthesis by carbidopa, which is a potent inhibitor of AADC activity

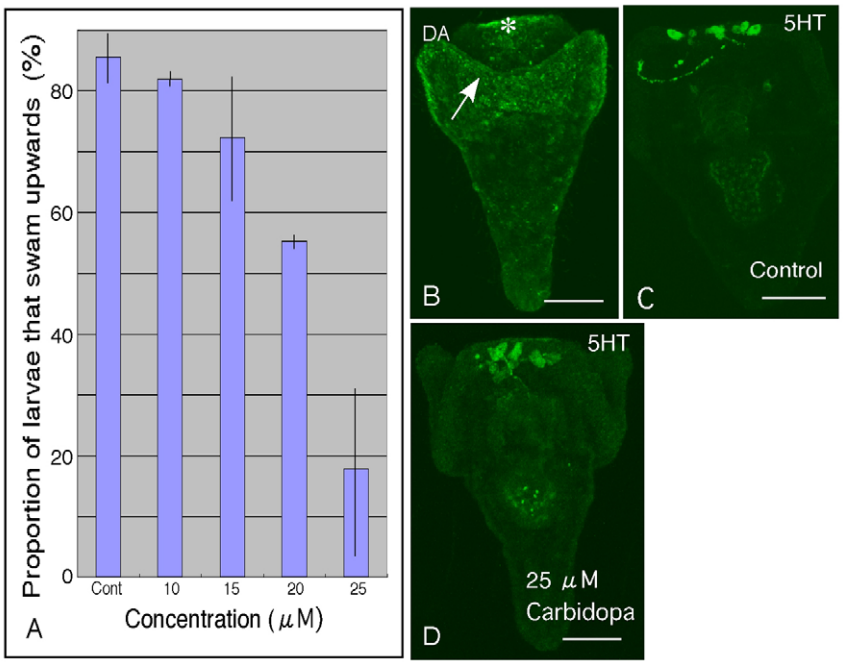

Fig. 9. Effects of carbidopa treatment, started at the 24 hpf prism larva stage and assayed at the 48 hpf pluteus stage. (A) Treatment with carbidopa from 15 to 25 μmol l^{-1} clearly decreased the swimming activity of larvae in a dose-dependent manner (Student's paired two-tailed *t*-test, $P<0.05$). Ordinate: percentage of larvae that swam upwards. A decrease in swimming activity was not obvious at concentrations less than 15 μmol l^{-1} ($P<0.5$). Abscissa: concentration of carbidopa. Cont, control. Error bars indicate s.d. (B) Immunohistochemistry for DAGs in a 48 hpf pluteus treated with 25 μmol l^{-1} carbidopa. DAGs at the ciliary band region (arrow) and the apical tuft region (asterisks) were obscure. (C) Serotonergic apical ganglion in a control pluteus. (D) Serotonergic apical ganglion in a pluteus treated with 25 μmol l^{-1} carbidopa. Scale bars: B–D, 50 μm.

that can affect the synthesis of serotonin and formation of the 5HT-NS. Although AADC is involved in the synthesis of both DA and serotonin (for a review, see Nagatsu, 1991), our findings indicate that inhibition of AADC by carbidopa did not inhibit serotonin synthesis. Thus, the decreased swimming activity of larvae treated with carbidopa is due to the decreased synthesis of DA.

DA and serotonin have been thought to have counteracting functions in the beating of cilia and/or the regulation of swimming activity (Braubach et al., 2006; Martin et al., 2008), because DA was shown to suppress the beating of cilia in the gill of the mollusk *Mytilus edulis* (Catapane et al., 1979) as well as that in the palatine mucosa of frog (Maruyama et al., 1983). However, in sea urchin larvae (Soliman, 1983b), as well as in the motile cilia that line the foot of the mollusk *Tritonia diomedea* (Woodward and Willows, 2006), both serotonin and DA have been shown to stimulate the beating of cilia. Our present observation that the suppression of DA synthesis results in decreased swimming activity in embryos and larvae and our previous observation that the suppression of serotonin synthesis results in decreased swimming activity in larvae (Yaguchi and Katow, 2003) are supported by previous reports (Soliman, 1983b; Woodward and Willows, 2006). These apparently contradictory results might indicate the presence of a tissue-specific mechanism to regulate the beating of cilia. In this scenario, both serotonin and DA could have opposite effects depending on the

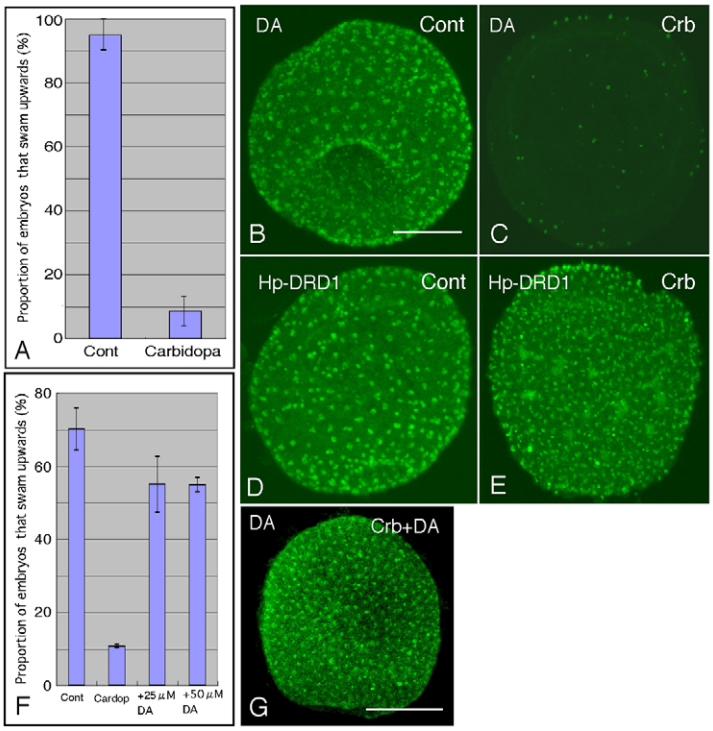

Fig. 10. Effects of carbidopa treatment, started soon after fertilization and assayed at the 20 hpf early gastrula stage. (A) Swimming activity was decreased considerably by treatment with 25 μmol l^{-1} carbidopa (Student's paired two-tailed *t*-test, $P<0.05$). Ordinate: percentage of embryos that swam up. Error bars indicate s.d. (B) Immunohistochemistry for dopamine (DA) in control gastrulae. (C) Gastrulae treated with 25 μmol l^{-1} carbidopa (Crb) showed a considerable decrease in the number of DA granules. (D) Immunohistochemistry for Hp-DRD1 in control gastrulae. (E) Gastrulae treated with 25 μmol l^{-1} carbidopa expressed DRD1 granules. (F) Despite the presence of 25 μmol l^{-1} carbidopa (cardop), swimming activity was almost completely restored in the presence of 25 μmol l^{-1} or more of exogenous DA. (G) Formation of DA granules was restored in the presence of 25 μmol l^{-1} DA. Scale bars in B and G, 50 μm.

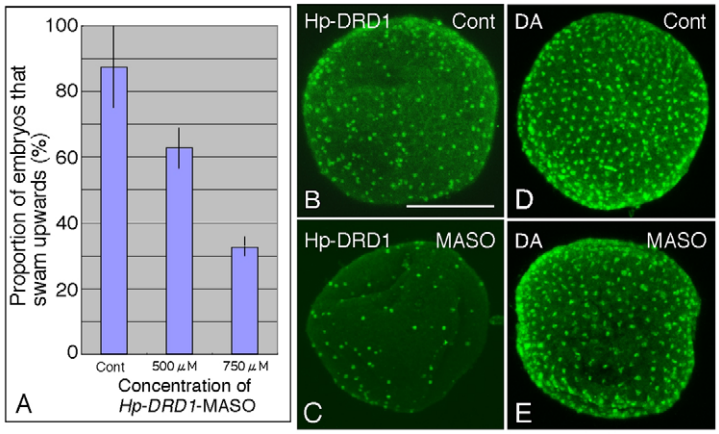

Fig. 11. Effects of injection of *Hp-DRD1*-MASO (MASO) into 20 hpf early gastrulae. (A) Dose-dependent decrease in the swimming activity of early gastrulae after MASO injection. Larval swimming decreased markedly at 750 μmol l^{-1} MASO (Student's paired two-tailed *t*-test, $P<0.05$), and to a lesser degree at 500 μmol l^{-1} ($P<0.5$). Ordinate: percentage of larvae that swam up. Abscissa: MASO concentration. Error bars indicate s.d. (B) Immunohistochemistry for Hp-DRD1 in a gastrula injected with 750 μmol l^{-1} standard control MASO. (C) A gastrula injected with 750 μmol l^{-1} MASO showing a considerable decrease in the number of DRD1 granules. (D) Immunohistochemistry for dopamine in a gastrula injected with 750 μmol l^{-1} standard control MASO. (E) A gastrula injected with 750 μmol l^{-1} MASO showing dopamine granules. Scale bar, 50 μm.

concentrations of the compounds to which cilia are exposed (Soliman, 1983b). On the other hand, our immunohistochemical results suggest a synergistic relationship between the 5HT-NS, SRCN and the preneural dopaminergic system. In early plutei, serotonin that is injected into the blastocoel triggers the release of calcium ions in the cytoplasm of ectodermal cells (Katow et al., 2007); therefore, physical contact between the 5HT-NS and SRCN might not be essential.

Although dopaminergic cells have been reported to exist from the four-arm pluteus stage, be found in the lower lip ganglion and the post-oral arm ganglia, and possess axonal connections (Bisgrove and Burke, 1987), our whole-mount immunohistochemistry conducted using two different anti-DA antibodies did not detect these structures. In our study, ectodermal cells that contained DA/DRD1-Gs had neither cytoplasmic DA nor axonal connections in embryos or larvae. These data suggest that DA is responsible for a preneural form of signal transduction, which contradicts a previous report on *S. droebachiensis* (Bisgrove and Burke, 1987). These discrepancies could be the result of differences between the species.

Although no immunohistochemical observation of a close localization between the DA/DA receptor and the basal body of cilia in organisms other than the present sea urchin embryos and larvae has been made to date, such sub-cellular localization and previously identified morphological and functional relationships may provide the morphological basis of DA involvement in the regulation of the beating of cilia through DA receptors (Catapane et al., 1979; Soliman, 1983b; Maruyama et al., 1983; Braubach et al., 2006; Martin et al., 2008).

Formation and sub-cellular localization of DA/DRD1-Gs

The results reported here could represent the first observation of the association of DA with granules that measure several micrometers in diameter. However, the association of Hp-DRD1 with such granules shows remarkable similarity to previous immunohistochemical findings on several subtypes of DA receptors in the human brain (Kumar and Patel, 2007) and multiciliated ependyma in rat, mouse and bovine species (Tomé et al., 2007). The observed DA/DRD1-Gs are far larger than a single GPCR protein (Cherezov et al., 2007), which suggests that each DA/DRD1-G is composed of multiple heteropolymers of components of the DA/DRD1 signaling pathway (Capasso et al., 1988; Carginale et al., 1992; Girault and Greengard, 2004; Arguello and Gogos, 2008).

We observed that DA and Hp-DRD1 appeared in granules on the surface of the ectoderm from the 9.5 hpf unhatched rotatory blastula stage until the end of the larval stages. Thus there was an apparent discrepancy between the continuous presence of *Hp-DRD1* mRNA from the unfertilized egg stage and the detection of Hp-DRD1 protein only from the 9.5 hpf unhatched blastula stage. The results obtained by RT-PCR were consistent with the pattern of accumulation of *Sp-DRD1* mRNA that was detected by microarray analysis (http://urchin.nidcr.nih.gov/cgi-bin/exp.plx?glean=11320). The DA binding site of DRD1 is located in the transmembrane domain, and it has been suggested that binding of DA to this site is associated with allosteric conformational change (Missale et al., 1998). However, the present study strongly suggests that the formation of DAGs and DRD1 granules occurs mechanically independently. Allosteric conformational change of the DRD1 molecule may not contribute to the acquisition of immunoreactivity. The mechanism underlying this phenomenon is yet to be found.

Although double-immunostaining for DA and Hp-DRD1 was not possible, the spatial relationship between DAGs and DRD1 granules that was detected by DA/γ-tubulin and Hp-DRD1/γ-tubulin double-staining strongly suggests that DAG is located close to DRD1 granules at the basal bodies of cilia. This suggests a close relationship between DA/DRD1-Gs and the beating of cilia, and hence to the swimming of embryos and larvae.

ACKNOWLEDGEMENTS

We thank M. Washio for collecting the sea urchins for this study and Dr Y. Nakajima for generously providing us with the 1E11 antibody.

LIST OF SYMBOLS AND ABBREVIATIONS

AADC	aromatic-L-amino acid decarboxylase
AT	acetylated tubulin
BrdU	5′-bromo-2′-deoxyuridine
DA	dopamine.
DA/DRD1-G	dopamine/DRD1 granule
DAGs	dopaminergic granules
dpf	days post-fertilization
FSW	filtered seawater
5HT-NS	serotonergic nervous system
GPCRs	G-protein-coupled receptors
GST	glutathione S-transferase
HNPGs	half number of positive granules
Hp-DRD1	*Hemicentrotus pulcherrimus* homolog of the dopamine receptor 1
hpf	hours post-fertilization
L-DOPA	L-3,4-dihydroxyphenylalanine
MASO	morpholino antisense oligonucleotides
PBST	phosphate-buffered saline with 0.1% Tween-20
*p*CPA	*para*-chlorophenylalanine
PI	propidium iodide
RT-PCR	reverse transcriptase polymerase chain reaction
SRCN	serotonin receptor cell network
Syn-NS	anti-synaptotagmin antibody-positive nervous system

REFERENCES

Anitole-Misleh, K. G. and Brown, K. M. (2004). Developmental regulation of catecholamine levels during sea urchin embryo morphogenesis. *Comp. Biochem. Physiol. A Physiol.* **137**, 39-50.

Arguello, P. A. and Gogos, J. A. (2008). A signaling pathway AKTing up in schizophrenia. *J. Clin. Invest.* **118**, 2018-2021.

Bisgrove, B. W. and Burke, R. D. (1987). Development of the nervous system of the pluteus larva of *Strongylocentrotus droebachiensis*. *Cell Tissue Res.* **248**, 335-343.

Braubach, O. R., Dickinson, A. J., Evans, C. C. and Croll, R. P. (2006). Neural control of the velum in larvae of the gastropod, *Ilyanassa obsoleta*. *J. Exp. Biol.* **209**, 4676-4689.

Capasso, A., Parisi, E., De Prisco, P. and De Petrocellis, B. (1987). Catecholamine secretion and adenylate cyclase activation in sea urchin eggs. *Cell Biol. Int. Rep.* **11**, 457-463.

Capasso, A., Creti, P., De Petrocellis, B., De Prisco, P. P. and Parisi, E. (1988). Role of dopamine and indolamine derivatives in the regulation of the sea urchin adenylate cyclase. *Biochem. Biophys. Res. Commun.* **154**, 758-764.

Carginale, V., Borrelli, L., Capasso, A. and Parisi, E. (1995). Changes in dopamine uptake and developmental effects of dopamine receptor inactivation in the sea urchin. *Mol. Reprod. Dev.* **40**, 379-385.

Carginale, V., Capasso, A., Madonna, L., Borrelli, L. and Parisi, E. (1992). Adenylate cyclase from sea urchin eggs is positively and negatively regulated by D-1 and D-2 dopamine receptors. *Exp. Cell Res.* **203**, 491-494.

Castella, P., Sawai, S., Nakao, K., Wagner, J. A. and Caudy, M. (2000). HES-1 repression of differentiation and proliferation in PC12 cells: Role for the helix 3-helix 4 domain in transcription repression. *Mol. Cell. Biol.* **20**, 6170-6183.

Catapane, E. J., Stefano, G. B. and Aiello, E. (1979). Neurophysiological correlates of the dopaminergic cilio-inhibitory mechanism of *Mytilus edulis*. *J. Exp. Biol.* **83**, 315-323.

Cherezov, V., Rosenbaum, D. M., Hanson, M. A., Rasmussen, S. G. F., Thian, F. S., Kobilka, T. S., Choi, H.-J., Kuhn, P., Weis, W. I., Kobilka, B. K. et al. (2007). High-resolution crystal structure of an engineered human β_2-Adrenergic G protein-coupled receptor. *Science* **318**, 1258-1265.

De Bremaeker, N., Baguet, F. and Mallefet, J. (2000). Effects of catecholamines and purines on luminescence in the brittlestar *Amphipholis squamata* (Echinodermata). *J. Exp. Biol.* **203**, 2015-2023.

Gilbert, J. A., Frederick, L. M. and Ames, M. M. (2000). The aromatic-L-amino acid decarboxylase inhibitor carbidopa is selectively cytotoxic to human pulmonary carcinoid and small cell lung carcinoma cells. *Clin. Cancer Res.* **6**, 4365-4372.

Girault, J.-A. and Greengard, P. (2004). The neurobiology of dopamine signaling. *Arch. Neurol.* **61**, 641-644.

Gustafson, T. and Toneby, M. (1970). On the role of serotonin and acetylcholine in sea urchin morphogenesis. *Exp. Cell Res.* **62**, 102-117.

Hadrys, T., DeSalle, R., Sagasser, S., Fischer, N. and Schierwater, B. (2005). The trichoplax PaxB gene: a putative proto-PaxA/B/C gene predating the origin of nerve and sensory cells. *Mol. Biol. Evol.* **22**, 1569-1578.

Hagiwara, H., Kano, A., Aoki, T., Ohwada, N. and Takata, K. (2000). Localization of gamma-tubulin to the basal foot associated with the basal body extending a cilium. *Histochem. J.* **32**, 669-671.

Huet, M. and Franquinet, R. (1981). Histofluorescence study and biochemical assay of catecholamines (dopamine and noradrenaline) during the course of arm-tip regeneration in the starfish, *Asterina gibbosa* (Echinodermata, Asteroidea). *Histochemistry* **72**, 149-154.

Inoue, M., Tamori, M. and Motokawa, T. (2002). Innervation of holothurian body wall muscle: inhibitory effects and localization of 5-HT. *Zool. Sci.* **19**, 1217-1222.

Kanoh, K., Aizu, G. and Katow, H. (2001). Disappearance of an epithelial cell surface-specific glycoprotein (Epith-1) associated with epithelial-mesenchymal conversion in sea urchin embryogenesis. *Dev. Growth Differ.* **43**, 83-95.

Kase, S., Yoshida, K., Ohgami, K., Shiratori, K., Ohno, S. and Nakayama, K. I. (2006). Phosphorylation of p27 (KIP1) in the mitotic cells of the corneal epithelium. *Curr. Eye Res.* **31**, 307-312.

Katow, H., Yaguchi, S., Kiyomoto, M. and Washio, M. (2004). The 5-HT receptor cell is a new member of secondary mesenchyme cell descendants and forms a major blastocoelar network in sea urchin larvae. *Mech. Dev.* **121**, 325-337.

Katow, H., Yaguchi, S. and Kyozuka, K. (2007). Serotonin stimulates $[Ca^{2+}]_i$ elevation in ciliary ectoderm cells of echinoplutei through a serotonin receptor cell network in the blastocoel. *J. Exp. Biol.* **210**, 403-412.

Katow, H., Elia, L. and Byrne, M. (2009). Development of nervous systems to metamorphosis in feeding and non-feeding echinoid larvae, the transition from bilateral to radial symmetry. *Dev. Genes Evol.* **219**, 67-77.

Kumar, U. and Patel, S. C. (2007). Immunohistochemical localization of dopamine receptor subtypes (D1R-D5R) in Alzheimer's disease brain. *Brain Res.* **1131**, 187-196.

Lacalli, T. C. and West, J. E. (1986). Ciliary band formation in the doliolaria larva of *Florometra*. *J. Embryol. Exp. Morphol.* **96**, 303-323.

Martin, K., Huggins, T., King, C., Carroll, M. A. and Catapane, E. J. (2008). The neurotoxic effects of manganese on the dopaminergic innervation of the gill of the bivalve mollusc, *Crassostrea virginica*. *Comp. Biochem. Physiol. C Pharmacol. Toxicol. Endocrinol.* **148**, 152-159.

Maruyama, I., Yamamoto, T., Ochi, J., Nakai, Y. and Yamada, S. (1983). Dopaminergic innervation and inhibition of ciliary movement in the ciliated epithelium of frog palatine mucosa. *Eur. J. Pharmacol.* **90**, 325-331.

Missale, C., Nash, S. R., Robinson, S. W., Jaber, M. and Caron, M. G. (1998). Dopamine receptors: from structure to function. *Physiol. Rev.* **78**, 189-225.

Muresan, V., Joshi, H. C. and Besharse, J. C. (1993). Gamma-tubulin in differentiated cell types: localization in the vicinity of basal bodies in retinal photoreceptors and ciliated epithelia. *J. Cell Sci.* **104**, 1229-1237.

Nagatsu, T. (1991). Genes for human catecholamine-synthesizing enzymes. *Neurosci. Res.* **12**, 314-345.

Ooka, S., Katow, T., Yaguchi, S., Yaguchi, J. and Katow, H. (2010). Spatiotemporal expression of an encephalopsin ortholog of the sea urchin *Hemicentrotus pulcherrimus* (Hp-ECPN) during early development, and its potential role in larval vertical migration. *Dev. Growth Differ.* **52**, 195-207.

Showman, R. M. and Foerder, C. A. (1979). Removal of the fertilization membrane of sea urchin embryos employing aminotriazole. *Exp. Cell Res.* **120**, 253-255.

Soliman, S. (1983a). Pharmacological control of ciliary activity in the young sea urchin larva. Effects of cholinergic and anticholinergic agents. *Comp. Biochem. Physiol. C Pharmacol. Toxicol. Endocrinol.* **74**, 397-407.

Soliman, S. (1983b). Pharmacological control of ciliary activity in the young sea urchin larva. Effects of monoaminergic agents. *Comp. Biochem. Physiol. C Pharmacol. Toxicol. Endocrinol.* **76**, 181-191.

Steffen, W., Fajer, E. A. and Linck, R. W. (1994). Centrosomal components immunologically related to tektins from ciliary and flagellar microtubules. *J. Cell Sci.* **107**, 2095-2105.

Stephens, R. E. (2008). Ciliogenesis, ciliary function, and selective isolation. *ACS Chem. Biol.* **3**, 84-86.

Strathmann, R. R. (2007). Time and extent of ciliary response to particles in a non-filtering feeding mechanism. *Biol. Bull.* **212**, 93-103.

Suyemitsu, T. (2007). Role of the dopamine receptor on the metamorphosis of sea urchin larvae. *SUCRA* **5**, 666-667.

Tomé, M., Moreira, E., Pérez-Fígares, J.-M. and Jiménez, A. J. (2007). Presence of D_1- and D_2-like dopamine receptors in the rat, mouse and bovine multiciliated ependyma. *J. Neural Transm.* **114**, 983-994.

Toneby, M. (1980). Dopamine in developing larvae of the sea urchin *Psammechinus miliaris* GMELIN. *Comp. Biochem. Physiol. C Pharmacol. Toxicol. Endocrinol.* **65**, 139-142.

Voronezhskaya, E. E., Hiripi, L., Elekes, K. and Croll, R. P. (1999). Development of catecholaminergic neurons in the pond snail, *Lymnaea stagnalis*: I. Embryonic development of dopamine-containing neurons and dopamine-dependent behaviors. *J. Comp. Neurol.* **404**, 285-296.

Woodward, O. M. and Willows, A. O. (2006). Nervous control of ciliary beating by Cl^-, Ca^{2+} and calmodulin in *Tritonia diomedea*. *J. Exp. Biol.* **209**, 2765-2773.

Yaguchi, S. and Katow, H. (2003). Expression of *tryptophan 5-hydroxylase* gene during sea urchin neurogenesis and role of serotonergic nervous system in larval behavior. *J. Comp. Neurol.* **466**, 219-229.

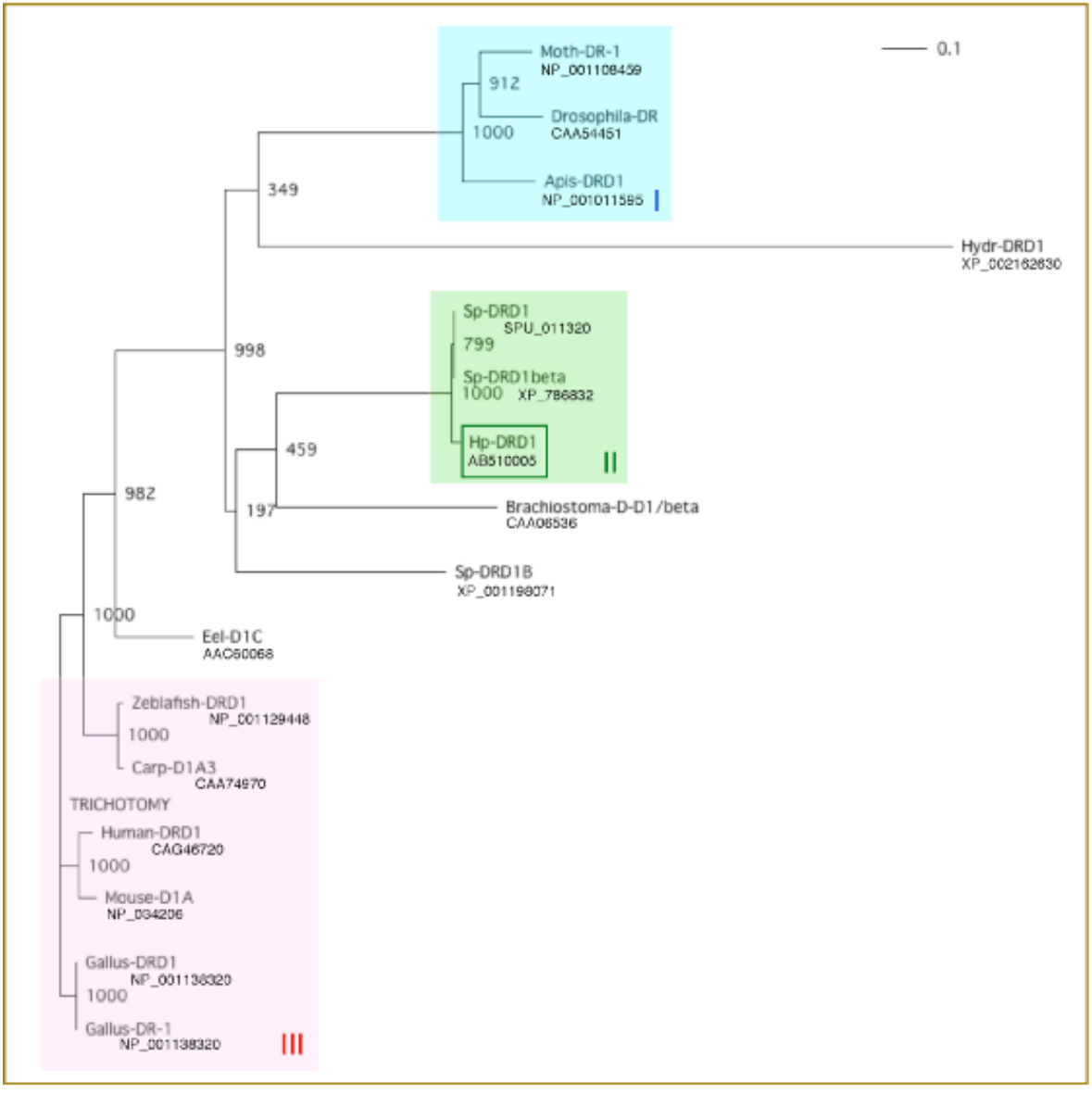
0.1
Moth-DR-1
NP_001108459
912
Drosophila-DR
CAA54451
1000
Apis-DRD1
NP_001011585
349
Hydr-DRD1
XP_002162830
Sp-DRD1
SPU_011320
799
Sp-DRD1beta
1000 XP_786832
Hp-DRD1
AB510005
998
459
982
197
Brachiostoma-D-D1/beta
CAA06536
Sp-DRD1B
XP_001199071
1000
Eel-D1C
AAC60068
Zebrafish-DRD1
NP_001129448
1000
Carp-D1A3
CAA74970
TRICHOTOMY
Human-DRD1
CAG46720
1000
Mouse-D1A
NP_034206
Gallus-DRD1
NP_001138320
1000
Gallus-DR-1
NP_001138320